Badger Andrew (Orcid ID: 0000-0003-4537-9993)
Bjarke Nels (Orcid ID: 0000-0002-0006-1060)

The sensitivity of runoff generation to spatial snowpack uniformity in an alpine watershed: Green Lakes Valley, Niwot Ridge Long Term Ecological Research Station

GLV runoff sensitivity to snowpack uniformity

A. M. Badger[1,2], N. Bjarke[3], N. P. Molotch[4,5,6], and B. Livneh[3,7]

[1]Universities Space Research Association, Columbia, MD, USA
[2]NASA Goddard Space Flight Center, Greenbelt, MD, USA
[3]Department of Civil, Environmental and Architectural Engineering, University of Colorado Boulder, Boulder, CO, 80309.
[4]Department of Geography, University of Colorado Boulder, Boulder, CO, 80309.
[5]Institute of Arctic and Alpine Research, University of Colorado Boulder, Boulder, CO, 80309.
[6]Jet Propulsion Laboratory, California Institute of Technology, Pasadena, CA, 91109
[7]Cooperative Institute for Research in Environmental Science (CIRES), University of Colorado Boulder, Boulder, CO, 80309.

Corresponding author: Andrew M. Badger (andrew.m.badger@nasa.gov)

Acknowledgments
This research was supported by funding from the National Science Foundation's Division of Environmental Biology (NSF / DEB 1027341). Completion of this work was partially supported by NOAA Grant # NA15OAR4310144; NOAA Grant# NA16OAR4310132; NOAA Grant# NA19OAR4310284; and NASA Grant # 80NSSC17K0017. The authors would like to thank Leanne Lestak for their help in gathering input data for the model setup.

Conflict of Interest Statement
The authors declare no conflict of interest.

The sensitivity of runoff generation to snowpack distribution uniformity in an alpine watershed: Green Lakes Valley, Niwot Ridge Long Term Ecological Research Station

Abstract
Seasonal water storage in high-elevation alpine catchments are critical sources of water for mountainous regions like the western U.S. The spatial distribution of snow in these topographically complex catchments is primarily governed by orography, solar radiation, and wind redistribution. While the effect of solar shading is relatively consistent from year-to-year, the redistribution of snow due to wind is more variable—capable of producing snowpacks that have varying degrees of uniformity across these hydrologically-important catchments. A reasonable hypothesis is that a warmer climate will cause snowfall to become more dense (i.e. wetter and heavier), possibly leading to less wind redistribution and thus produce a more uniformly distributed snowpack across the landscape. In this study, we investigate the role of increasingly uniform spatial snowpack distributions on streamflow generation in the Green Lakes Valley Niwot Ridge Long Term Ecological Research station, within the headwaters of the Boulder Creek watershed in Colorado. A set of idealized hydrologic simulation experiments driven by reconstructed snowpacks spanning 2001-2014 show that more a more uniform spatial snowpack distribution leads to an earlier melt-out of 31 days on average and tends to produce less total streamflow, with maximum decreases as large as 7.5%. Isolating the role of snowpack heterogeneity from melt-season precipitation, we find that snowpack uniformity reduces total streamflow by as much as 13.2%. Reductions in streamflow are largely explained by greater exposure to solar radiation in the uniformly distributed case relative to a more heterogeneous snowpack, with this exposure driving shifts towards earlier snowmelt and changes in soil water storage. Overall, we find that the runoff efficiency from shallower snowpacks is more sensitive to the effects of uniformity than deeper snowpacks, which has potential implications for a warming climate where shallower snowpacks and enhanced sensitivities may be present.

Keywords
Snowpack uniformity, Streamflow, Runoff, Sensitivity, Hydrologic model, Alpine catchment, Snowmelt, Niwot Ridge LTER

1. Introduction

Mountain regions can be understood as the world's 'water towers' (Immerzeel et al., 2010) as more water disproportionately originates from these regions than adjacent lowlands (Viviroli et al., 2007) with water largely exported as snowmelt. Observed regional warming in the last several decades endangers this vital natural reservoir of surface water storage by altering the timing and rate of snowmelt (Clow, 2010; Stewart, 2009), but changes to the efficiency of snowmelt runoff production is dependent on more complex water-energy fluxes at the regional and catchment scales (Hartman et al., 1999; Knowles et al., 2015; Luce et al., 1998, Barnhart et al., 2016). A specific knowledge gap is how the impacts of warming driven changes in snowpack spatial heterogeneity will affect runoff generation from these important areas. In this respect, future warming and increases in snowfall density may increase spatial uniformity of snowpacks due to less wind redistribution. In this manuscript, we investigate the impact of greater spatial snowpack uniformity on snowmelt-driven runoff efficiency in the high alpine Green Lakes Valley catchment part of the Niwot Ridge Long-Term Ecological Research (LTER) site.

In the western United States, observed changes in alpine snowpack and snowmelt timing associated with warming climate (Cayan, 1996; Clow, 2010; Hamlet et al., 2005; Mote et al., 2005; Stewart, 2009) have implications for the future of water resources systems that depend on snow as a natural reservoir for storage (Rajagopalan et al., 2009; Vano, 2020). Alpine environments, such as the Green Lakes Valley in the headwaters of Boulder Creek watershed in Colorado, have been described as among the most vulnerable to climate change (Jones et al., 2012; Field et al., 2014). The Green Lakes Valley is already experiencing shifts towards earlier peak snowmelt (Greenland, 1989; Kittel et al., 2015; Knowles et al., 2015; McGuire et al., 2012) consistent with the snowmelt timing trends of the western US more broadly, though temperature increase is not the sole driver of changes to snowmelt and subsequent runoff (Hartman et al., 1999; Luce et al., 1998). The timing and volume of snowmelt within an ablation season is dependent on a number of physical factors, in addition to increasing temperatures, including rain on snow events (Marks et al., 2001; McCabe et al., 2007), dust on snow events (Deems et al., 2013; Livneh et al., 2015), and the spatial distribution of snow (Luce et al., 1998, 1999).

Critically, these drivers of snowmelt also modulate the runoff efficiency of alpine catchments by altering the timing and spatial distribution of catchment water inputs.

After snow is deposited on the ground, the distribution of snowpack across alpine catchments is primarily dependent on wind transport (Elder et al., 1991; Essery et al., 1999; Kane et al., 1991a; Pomeroy, 1991), solar radiation (Pomeroy et al., 2003), topographic organization (Elder et al., 1991), orographic effects (Barros & Lettenmaier, 1994; Fontaine et al., 2002), and gravitational transport (Freudiger et al., 2017). Of the physical mechanisms that control the distribution of snowpack, wind-driven redistribution is unique in both its interannual variability and its sensitivity to the composition of the existing snowpack (Li & Pomeroy, 1997). Higher temperatures have potential to decrease the lateral transport and redistribution of snow by wind due to the associated increase in snowpack density and wetness (Judson & Doesken, 2000). Mechanically, Doorschot et al. (2004) and Clifton et al. (2006) find that liquid water enables snow grains to adhere to one another more easily, increasing the wind speed needed to transport increasingly wet and dense snow. Li and Pomeroy (1997) further explain that wet snow needs significantly higher wind speeds for transport because of the viscous forces corresponding to the liquid water adhering the snow grains. This decrease in lateral transport of snow is one of the potential changes to mountain snowpack within a changing climate (Guyomarc'h & Mérindol, 1998; Li & Pomeroy, 1997) and is of primary interest for this analysis. Specifically, reduction of wind transport of snow across the landscape may result in more uniformly distributed snowpacks across alpine catchments, which has the potential to alter the amount of runoff produced during the snowmelt season (Hartman et al., 1999; Liston, 1999; Luce et al., 1998)

Previous investigations into the effect of snowpack spatial variability have used observations (Kane et al., 1991b) and hydrologic models (Hartman et al., 1999), showing a positive relationship between the spatial variability of snowpack and the runoff ratio. However, complexity in the process-based simulations of wind redistribution of snow (Essery et al., 1999; Essery & Etchevers, 2004; Li & Pomeroy, 1997; Pomeroy, 1991; Winstral et al., 2002) leads to simulations of snow distribution that do not accurately predict observed snowpack distribution, particularly in complex alpine terrain (Fontaine et al., 2002; Winstral et al., 2002). So, while there is value in modeling the redistribution of snow, adding such a complex element may not be

necessary to study hydrologic impacts of snowpack distribution; regardless of model complexity, the ability to accurately simulate wind distribution of snow is a difficult task in such mountainous and complex topography. However, through the manual redistribution of snow, the effects of reduced wind redistribution can be seen in a hydrologic model with more experimental control and fewer uncertainties introduced.

In this paper, we use the Distributed Hydrology Soil Vegetation Model (DHSVM) to investigate the sensitivity of streamflow production to snowpack spatial variability in the Green Lakes Valley (GLV), Colorado. We initialize melt-season model simulations with spatial snow distributions of increasingly uniform snowpacks relative to a control case that is reflective of historical conditions at the time of peak snow water equivalent (SWE). The runoff efficiency – the amount of runoff generated from a unit of water input - is evaluated as a way to quantify the effects of spatial snowpack uniformity on subsequent snowmelt generated runoff. Simulations with and without warm season precipitation are generated in order to further isolate the effects of the initial snow distribution on surface water generation from confounding processes that modulate snowmelt rate during the ablation season. This fills an important knowledge gap by directly evaluating the role of the initial state of the snowpack distribution uniformity on melt-season streamflow generation, an important topic for a broad audience of water resource managers and hydrologists, given the projected increases in regional temperatures over the western US in the coming decades that could potentially alter snow redistribution due to wind.

2. Materials and Methods

We begin by describing the study domain (Sec. 2.1), followed by model inputs and parameter settings (Sec. 2.2). The experimental design (Sec. 2.3) is constructed with the goal of evaluating how increasingly uniform snow distributions affect runoff efficiency relative to an observation-based historical control simulation.

2.1 Study domain

This study focuses on the GLV, located within the U.S. National Science Foundation Niwot Ridge LTER site (Figure 1). The GLV is located approximately 35 km west of Boulder, Colorado, bounded on the western-side by the Continental Divide, with the eastward outflow

representing a primary water source for the city of Boulder, CO. The GLV is a relatively small alpine catchment with an area of 2.3 km^2, but with topographic relief spanning elevations of 3250 m to 3798 m. The annual mean temperature of the region is -3.8°C (Williams et al., 1996) and Caine (1996) notes that the region receives approximately 1000 mm of precipitation annually, nearly 80% of which falls as snow that accumulates from October to April. Being a snowmelt dominated basin, runoff derived from snowmelt accounts for approximately 70% of the total annual runoff at the basin gauge (40.049°N, -105.617°E), peaking between late-April and mid-July (Caine, 1996).

2.2 Model Description

The Distributed Hydrology Soil and Vegetation Model (DHSVM; Wigmosta et al., 1994) was chosen given its development towards simulating hydrology in steep mountain catchments. DHSVM's treatment of relatively fine scale hydrologic processes, e.g. dynamic lateral routing, makes the model uniquely suited for simulating streamflow in topographically complex domains (Whitaker et al., 2003; Brooks et al., 2004; Livneh et al., 2014, 2015). The model has an intermediate complexity snow model (Raleigh et al., 2016) that resolves a two-layer energy balance model for snow accumulation and snowmelt. Soil moisture and surface runoff are computed via a multilayer unsaturated soil model and a saturated subsurface flow model. Energy transfer and evapotranspiration (ET) are computed via a two-layer canopy representation. The model considers the influences of slope and aspect on incoming radiation (shortwave and longwave) within the surface energy budget.

In this analysis, DHSVM was configured to run at an hourly time step from 2001 to 2014 at a 20 m horizontal resolution. These settings were chosen based on the availability of model input data. DHSVM inputs include spatial fields of vegetation and monthly phenology, soil depth and texture, geology, and topography. Here, these gridded model fields reflect a combination of local observations from the Niwot Ridge LTER network and regional-to-national scale datasets (see Table 1). DHSVM is additionally provided dynamic observations for solar shading as well as a gridded estimate of the mean diurnal cycle of cloud free incoming solar radiation each month, derived from a digital elevation model (DEM) used in the model simulations.

Hourly time-series of meteorological information used to force DHSVM were derived from five observation locations within the Niwot Ridge domain (see Figure 1 and Table 2). The prescribed meteorological inputs for the model include downwelling shortwave and longwave radiation, humidity, wind speed, precipitation, air temperature, and soil temperature. Data continuity issues associated with power and instrument failures are a common issue with surface observations in extreme climates. To address data gaps associated with these issues, an infilling procedure similar to the normal ratio method (NRM; Xia et al., 1999) was performed on the basis of weighting station-to-station correlations to derive daily mean values for insertion of missing data. Meteorological variables are interpolated to all grid cells automatically within DHSVM using a Cressman scheme (Westrick and Mass, 2001) that can be informed by additional spatial covariates to distribute the local meteorology. A simulation period of water years 2001-2014 was chosen given the greatest number of high-quality meteorological observations available to drive DHSVM during the timeframe. It should be noted that DHSVM does not explicitly simulate changes to the prevailing climate, but rather the meteorological information used to force DHSVM can impose a changing climate. This study does not impose any changes to the climate signal (i.e. detrending, increased temperature) in the meteorological forcing, but observable trends in the climate may be present in the meteorological forcing.

The melt-season experiments are initialized to an observationally-based estimate of peak SWE targeted on May 1 (Figure 2a), which represents the climatological time of peak SWE for the GLV. The Jepsen et al. (2012) SWE reconstruction provides an estimate of the yearly maximum SWE by integrating modeled snowmelt from the date of maximum SWE to the date of observed disappearance using observed meteorology to estimate energy balance calculations. The 12-year climatological mean of the SWE reconstruction, 1996-2007, was used to aid in informing the Cressman scheme for interpolation of meteorological variables, such that the dynamic hydrologic simulations closely match the spatial pattern of the reconstruction on May 1 of each year, while allowing for interannual variability in the magnitude of total SWE and other hydrologic states like soil moisture each year.

While the Jepsen et al. (2012) SWE reconstruction implicitly accounts for wind redistribution based on the date of snow disappearance and energy inputs into the snowpack, DHSVM does not

explicitly model wind redistribution processes. Given the numerous uncertainties associated with snowpack wind-redistribution, we chose not to model wind redistribution, but instead to initialize melt-season simulations to a realistic pattern of spatial variability. Specifically, the model experiments (described in Sec. 2.3) assume a given spatial distribution derived from Jepsen et al. (2012) with the focus on modeling melt-season snowmelt and associated runoff fluxes under prescribed levels of spatial snowpack uniformity.

The majority of the DHSVM soil and snow parameters were obtained from a previous application over the Boulder Creek watershed (Livneh et al., 2014; 2015), since the Green Lakes Valley lies within this basin. Those past analyses demonstrated realistic simulation of snowmelt and streamflow dynamics. The Livneh et al. (2014; 2015) model set up is used here to provide initial settings for soil and vegetation parameters.

To optimize our calibration procedure, we used a two-step method for calibrating paraments. We initially determine the "directional sensitivity" of six DHSVM parameters – lateral conductivity (Kh), exponential decrease in Kh (Kexp), vertical conductivity (Kv), minimum resistance (MinRes), snow roughness (SnowR), and snow water content (SnowWC) – by multiplying the original parameter values by 0.25, 0.5, 2 and 4. Based on the results from the first step, we determined that Kh, Kexp and Kv were the most sensitive when reproducing streamflow. The next step was to use a set of Monte Carlo simulations for the multi-variate calibration with a Latin Hypercube (McKay et al., 1979) sampling method to get 256 combinations of parameters across a range of distributions for the selected parameters, with the selection criteria for the parameter settings being a maximum ranked correlation. Following a Monte Carlo search for the selected parameters, our chosen simulation provided a correlation of 0.838 and Spearman ranked correlation of 0.921 for all daily streamflow with the daily mean annual cycle (Figure A1) being 0.969 and 0.964 respectively, with the grey area in Figure A1 representing the series of Monte Carlo simulations for calibration. Due to potential errors in streamflow observation during the winter months when the gauge is covered by snow and ice, percent bias calculated during the melt-season (MJJ) and full warm-season (MJJAS) were -12.14% and -21.84%, respectively, suggesting satisfactory portrayal of daily streamflow estimates following the guidance of Moriasi et al. (2007). While the given biases do show some

deficiencies in the model under simulating total streamflow, this study does not aim to replicate observed streamflow but rather to understand the sensitivity to streamflow as snowpack distributions are altered.

2.3 Design of model experiments

For every year in the simulation period, six variations of initial May 1 SWE distributions were developed (Figure 2). Each variation had a progressively more uniformly distributed snowpack while conserving the same total basin mean SWE as in the control. In each smoothing increment, 1/6th of SWE depth was transferred from locations with greater SWE than in the control, to areas with below average SWE, while conserving the total basin mean SWE in all cases. It is of note that as SWE is redistributed, areas that were once barren (i.e. no snow) will now be snow-covered, which not only creates a more spatially uniform SWE, but increased the snow coverage in the catchment. This method ultimately produced a spatially uniform snowpack by the sixth iteration. Table 3 provides a simple measure of uniformity, U, computed for each snowpack distribution:

$$U = \frac{\sigma_{SWE}}{\mu_{SWE}} \qquad \text{(Equation 1)}$$

where σ_{SWE} is the spatial standard deviation of SWE and μ_{SWE} is the basin mean SWE. Smaller values of U correspond with increasing spatial uniformity for the initial snow conditions. The value of U scales linearly with the changing spatial standard deviation, given that the mean SWE remains constant in all cases.

Transferring snow from wetter areas to drier areas while conserving total catchment-wide SWE in this way enables the experiment to investigate the effects of wind redistribution on the resulting hydrology in a controlled way. Notably, this framework allows for a straightforward method to isolate the effects of the spatial snowpack distribution, while not introducing additional uncertainties associated with complex parameterizations that would be evident in a snow distribution model. Despite being motivated by first order principles of increased snow density from increased temperatures and subsequent reduction in wind redistribution, these are still primarily 'idealized' experiments of snow distribution impacts on hydrology, thus changes to snow density are not accounted for. This design was chosen in order to isolate the role

snowpack distribution uniformity and not introduce ancillary factors that could confound the basin response and complicate isolating the role of snowpack uniformity,

For each simulation year, model simulations were initialized to the seven May 1 SWE distributions (one control distribution and six modified distributions) and forced with the observed meteorological forcing for their respective water-year, i.e. from May 1 through September 30. This experimental design provides an ensemble (i.e. variations of respective smoothing for each initial condition) of hydrologic model simulations initialized with the control and altered snowpacks for each year, while driven by identical forcing. Because this approach was applied for multiple years, 2001-2014, it lets us analyze different amounts of total SWE and different amounts of water year precipitation for each year (Figure 3). Ultimately, this interannual variability in SWE and precipitation leads to interannual variability in streamflow generation from the GLV. This variability in the primary sources of streamflow (SWE and precipitation) is an artifact of the natural variability present in the local climate, which can have inherent impacts on the processes governing streamflow generation.

This study relies on direct observations of quantities such as streamflow and meteorology, as well as observationally-based reconstructions of peak SWE. Each of these contains observational uncertainty that are entrained within comparisons with model simulations, which also contain uncertainty. The observational products used in this analysis were not consistently available with quantitative estimates of their attendant uncertainties. Therefore, these uncertainties are implicitly carried through into the results and discussion sections which primarily focus on ensemble mean values to minimize the potential role of model uncertainty on the overall results.

For each ensemble of snow distributions, confidence intervals are calculated from an empirically bootstrapped, 1000-member ensemble of daily SWE and runoff resampled from the simulations at each time-step. Day-of-year mean SWE/runoff are calculated for each of the 1000 ensemble members, and, for each day of the year, the 2.5^{th} and 97.5^{th} percentiles of the distribution of daily. These bootstrapped means are presented in the results as measure of model uncertainty for the simulation ensembles of each spatial snowpack distribution.

3. Results

The simulations of the various snowpack distributions highlight a few notable findings. First, the seasonal snowmelt pulse directly corresponds with the seasonal rise in runoff as is expected for this snowmelt dominated basin, however the increasingly uniformly distributed snowpacks melt at a more rapid rate than the control, as is seen in their sharper initial decline in Figure 4. In the control case, the melt-out of the snowpack (defined here as the first instance of basin mean SWE dropping to less than 5% of the respective May 1 SWE) occurs an average of 93 days (August 2) after May 1 model initialization. In contrast, the uniform snowpack melts out after 62 days (July 1) on average, or 31 days earlier than the control simulation. Overall, the melt-out date was consistently earlier for increasing spatial uniformity relative to the control simulation. However, the response is highly non-linear. For example, when redistributing half of the SWE from deeper to shallow snowpacks, melt out was only 10 days earlier than the control simulation, whereas transferring the remaining half of the snow mass caused an earlier melt out by an additional 21 days.

The largest differences in streamflow occurred during the period of rapid snowmelt early in the melt-season (Figure 4c). Increased spatially uniform snowpacks show greater early-season streamflow generation. However, these streamflow anomalies importantly change sign towards the end of August on average, ultimately producing less cumulative streamflow as compared to the control distribution by the end of the water-year. The date of peak streamflow was minimally changed across snowpack distributions, with the uniform snowpack peaking only 8 days prior to the control. The uniformly distributed snowpack case results in only 1.1% less cumulative streamflow than the control case on average, with decreases as large as 7.5% in some years. It appears that the melt-season precipitation (i.e. seen in Fig-3) provides uneven inputs of water into the catchment from year-to-year, which masks the effects of snowpack spatial uniformity on total runoff.

3.1 Model simulations in the absence of melt-season precipitation

To isolate the relationship between snowpack distribution uniformity and snowmelt from the confounding factor of variability in melt-season precipitation, we performed a set of additional simulations in an identical manner to the initial simulations, except precipitation forcings are

removed (i.e. set to zero) for the remainder of the post-May 1 water-year. Teufel et al. (2017) note that rain-on-snow events in the presence of frozen and snow-covered ground can lead to increased streamflow generation, a potential phenomenon that could obfuscate the role of spatial snowpack uniformity. We hypothesize that the subsequent delivery of precipitation (Figure 3) during the melt-season (e.g. amount, duration, intensity) is altering the manner in which the snowpacks are producing streamflow on a year-to-year basis.

The removal of melt-season precipitation forcing in Figure 5 shows the same hallmarks as in Figure 4 with more rapid snowmelt for increasingly uniform snowpack distributions. Changes in the melt-out date are similar for this new set of simulations, with a difference of 32 days between the control and uniform distributions. The mean snowpack melt-out date for all snow distributions is shifted roughly two weeks earlier (14 - 15 days) by the exclusion of melt-season precipitation. Importantly, the initial spatial snowpack uniformity influence on the timing of melt out, that is the difference melt out date between the control and uniform cases, is shown to be independent of the presence of melt-season precipitation.

The shape of the cumulative streamflow anomaly graph in Figure 5 is comparable to Figure 4, with the exception of clearer separation across experiments of increasingly uniform snowpack distributions. Compared with the 1.1% decline in Figure 4, in the absence of melt-season precipitation, there is an average decrease of 8.1% in total streamflow generation for the uniform distribution relative to the control distribution, a 7% difference from the previous set of simulations.

When melt-season precipitation forcing is withheld, spatially uniform snowpacks produce less cumulative streamflow for all cases relative to the control simulation (Figure 5c). Reductions by as much as 13.2% in total streamflow generation are computed when using the mean snowpack distribution, a reduction that is 12% greater than the ensemble mean of simulations that include melt-season precipitation.

The magnitude of the differences in cumulative runoff due to increasing degrees of snowpack spatial uniformity is most apparent in the simulations where the melt-season precipitation forcing

is withheld. That is, the melt-season precipitation dampens the signal of the spatially uniform snowpack initial condition on cumulative runoff such that, when melt-season precipitation is applied as a forcing in the simulations, the mean difference in cumulative runoff between cases of spatial uniformity falls within the uncertainty of the interannual variability of runoff. The removal of melt-season precipitation allows us to identify a distinct inverse relationship between the initial snowpack spatial uniformity condition and the subsequent cumulative runoff that is generated.

In contrast to the simulations that withhold melt-season precipitation, the previous simulations display instances when snowpacks with greater areal mean SWE increased streamflow for more uniform snowpack distribution. This finding suggests that deeper snowpack years may have experienced enhanced melt-season precipitation that confounded the role of spatial snowpack uniformity in the presence of precipitation. While in the absence of melt-season precipitation, the effect of snowpack uniformity in reducing streamflow displays a dependency with the magnitude of snowpack for a given year (Figure 6). Years with lower mean SWE appear more sensitive to increased snowpack uniformity and tend to produce larger percent decreases in streamflow generation. The implications of this sensitivity are important in the context of climate warming, where smaller future snowpacks may be more sensitive to increasingly uniform distributions than deeper historical snowpacks. While there does appear to be a slight trend towards larger snowpacks showing resilience to spatial snowpack uniformity, there is still variability from year-to-year. These differences largely occurred due to interannual variability in temperature and other forcings.

4. Discussion

Through the comparison of simulations with and without warm season precipitation, we find distinct changes in the streamflow generation for different levels of spatial snowpack uniformities. We further analyze our results to highlight the role of snowpack distributions and to propose a potential physical mechanism as to why changes in spatial uniformity impact streamflow generation.

4.1 Randomized snowpack distributions

Additional experiments were constructed to investigate the role of spatial uniformity on streamflow more generally. In this experiment, we shuffled the spatial snow patterns for the control and the other six redistributed snowpack initial conditions, to create 20 randomly generated distributions for each level of uniformity (Table 3), excluding the uniform case since all distributions would be the same. This approach was chosen because it keeps the degree of uniformity, U, constant for each set of 20 random samples, while altering the elevational distribution of SWE, the position of different depths of SWE relative to vegetation and topography, as well as the locations of minimum and maximum SWE within the basin. On average, the random distributions distribute snow more evenly throughout the basin, which has the effect of increasing the amount of snow at higher elevations (not shown) in comparison to the control-case, while also providing a wide-range of elevations for minimum and maximum SWE. Twenty random SWE distributions were generated at each level of spatial uniformity, from which DHSVM was run in the same manner as described in Section 2.3, to explore streamflow variation in response to this larger and more diverse sample of uniformity.

Figure 7 shows that each set of the randomized variations generally produces comparable results to the initial analysis, i.e., in Figure 5. Importantly, the randomized simulations reflect a range of altered elevation distributions of SWE, the amounts of SWE in shaded regions, and the general prevailing meteorology (i.e. air temperature) for different SWE depths. By altering all of these aspects through the randomization of SWE, the role of spatial uniformity is more robustly evaluated, which supports the finding that uniformity is driving changes in melt and streamflow production.

Further highlighting this point are the results from Winstral et al. (2002) in which a regression tree applied to model spatial snow distribution found wind redistribution to be a more important factor than elevation, solar radiation and slope of the terrain. The relative agreement on the factors that impact snow distribution as well as govern melt in our manuscript is generally consistent with our results on the role snowpack uniformity.

4.2 Discussion of physical mechanism

A comparison of water balance storage and surface flux terms (Figure 8) allows us to interpret physical mechanisms behind the sensitivities in runoff production associated with snow distribution. Here we focus on differences between the control and completely uniform simulations for periods before (i.e. when the uniform distribution produces more streamflow) and after (i.e. when the control distribution produces more streamflow) the inflection point in Figure 5.

A potential first-order explanation for why the uniformly distributed snowpack behaves differently is its larger surface area of snow exposed to surface-atmosphere energy exchange; e.g. incident solar and longwave radiation and sensible heat flux, leading to increased atmospheric exposure per unit SWE, it is worth noting that snow coverage increases due to redistribution (see Sec. 2.3). Given that snowmelt is driven at the surface-atmosphere interface, it is intuitive that a spatially uniform snowpack would generate more snowmelt earlier in the snowmelt season and less in the late season. Conversely, the control snowpack has both snow-free areas and areas of persistent deeper snow accumulated in snow drifts. Within these drifts a significant volume of total snowpack water storage is buried beneath surface layers of snow and is therefore not exposed to the overlying atmosphere. As the surface snowpack warms during the spring transition potential energy inputs to these deeper snowpack layers include conduction from overlying layers, advection from liquid water percolation, and latent heat exchange associated with re-freezing of vertically propagating liquid water. These energy sources are relatively small in comparison to the aforementioned energy inputs that are available at the surface-atmosphere interface. In addition, snowpack cold content varies as a function of snowpack temperature and SWE. Hence, deeper drifts in the control snowpack would have greater cold content than thinner, more uniformly distributed snowpacks and therefore delayed snowmelt is expected with more heterogeneous snowpacks. These differences are reflected in the increased snowmelt in the earlier period of Figure 8, where energy inputs more efficiently overcome the cold content of the uniform snowpack and lead to a larger early pulse of snowmelt.

In comparing the two time periods highlighted by Figure 8, the potential influence of the uniformly distributed snowpack's greater exposure to energy inputs per unit of SWE relative to the control case can be seen in water flux and storage terms. The early pulse of snowmelt in the uniform simulation leads to increases in soil moisture and decreases in the water-table depth (i.e. a water table closer to the surface), allowing for increased runoff efficiency and greater storage of water during the early season. While during the second time period when the control distribution produces more snowmelt due to deeper snow areas having longer melt times, there are opposite changes to all fluxes and storage terms.

Existing research has largely focused on broad-scale patterns in runoff from snowmelt-dominated watersheds, in comparison to rain-dominated watersheds (Berghuijs et al., 2014), as a function of time throughout the snow season (Barnhart et al., 2016, Musselman et al., 2017), or in the context of seasonal flood (Berghuijs et al., 2016) and drought prediction (Livneh and Badger, 2020). These studies generally rely upon large-scale models and data (~ 10 km scale), which are too coarse to resolve some of the important energy, water, and topographical forcings considered here, and so they only hint at dominant mechanisms.

In sum, we hypothesize that spatially uniform snowpacks melt more quickly due to greater energy exposure per unit of SWE, leading to increased runoff and storage in the land surface early in the season, while the slower melt rate from the control distribution provides a more efficient runoff generation that extends later into the melt-season.

4.3 Limitations and uncertainties

While the results in this study are based on use of a hydrologic model in a single alpine catchment, there could be elements of the results that are model and/or catchment dependent; further highlighting the need for comparable investigations into the streamflow changes due to the spatial uniformity of the initial melt-season snowpack.

Additionally, uncertainties due to meteorological forcing and snowpack reconstruction are present. Through the use of observed meteorology, there are inherent uncertainties associated with the collection and transmission of these data from remote locations such as the GLV; there

is general confidence in the data but using an in-filling method to address missing data periods can lead to observed features not being captured correctly. While accounting for interannual variability in meteorology, there is a lack of interannual variability in the pattern of the snowpack distributions, this is due to the lack of overlapping years with the SWE reconstruction product. Notwithstanding, previous works have highlighted that the patterns of SWE distribution have some interannual consistencies (Erickson et al., 2005; Jepsen et al., 2012).

Furthermore, removal of melt-season precipitation does allow for a more defined response to snowpack uniformity, but other elements of the observed meteorology that would be associated with a precipitation-free environment may be missed. Particularly, this study did not take into account the associated changes to incoming shortwave radiation, present wind speed, soil temperature and other aspects that could alter snowmelt dynamics in the absence of melt-season precipitation. Predicting associated changes to other meteorological variables in the absence of precipitation would have provided additional uncertainties to this study. While May 1 was chosen to represent the date of peak SWE following historical conditions, other initialization dates were not examined. A future exploration into SWE spatial uniformity across the melt season could be useful towards understanding sensitivities of runoff to uniformity through time.

Lastly, these results suggest that the magnitude effect of the initial snowpack spatial uniformity on cumulative runoff generation is comparable to the magnitude of interannual variability of melt-season precipitation. This underscores the importance of spatial snowpack uniformity in influencing total runoff. Furthermore, there is a strong consensus across projections of future regional temperature increases, i.e., the physical mechanism that is likely to drive increased spatial uniformity of snowpacks. In contrast, projections of spring and summer precipitation change are more uncertain, particularly in western North America (Hayhoe et al., 2018). In addition, these results indicate that initial spatial snowpack uniformity is directly proportional to the timing of melt out independent of the presence melt-season precipitation. Therefore, spatial

uniformity of snowpacks will remain an important consideration for water resource planning in snowpack dominated watersheds.

5. Conclusion

This study has investigated the role of spatial snowpack variability and potential uniformity in streamflow generation in the Green Lakes Valley watershed of the Niwot Ridge LTER. The DHSVM hydrologic simulations conducted here show that snowpacks with increased spatial uniformity are expected to reduce total streamflow relative to the control case, although melt-season meteorology can have confounding impacts on this signal. Snowpack uniformity leads to greater exposure to incoming solar radiation at the snowpack surface and enhances the rate of snowmelt for the catchment. More explicitly, these simulations showed consistently earlier melt-out dates independent of melt-out season precipitation, increased early season melt, decreased late season melt, reduced efficiency and ultimately decreased streamflow generation as a result of increasing snowpack uniformity. Importantly, these sensitivities appear to be heightened for shallower snowpacks, which has implications for climate change.

While these results are presented independent of a changing climate, the Niwot Ridge LTER is expected to experience such changes. Kittel et al. (2015) notes that there is an observed precipitation trend of 60 mm $year^{-1}$ $decade^{-1}$ for our domain, there is also an observed temperature trend of 0.8°C $decade^{-1}$ occurring simultaneously. A hypothesis worth addressing in future work could investigate the degree to which continued increases in precipitation could potentially offset the impact of increased temperature-driven evaporative demands on streamflow. While this region is experiencing increases in both precipitation and temperature, it is expected that other regions may warm with differing precipitation changes, such that resulting changes in streamflow generation could be investigated following a similar approach as was taken here.

Although this study investigated a single alpine catchment, the principles of snowpack spatial uniformity and greater solar exposure relative to more heterogeneous snowpacks are expected to influence the water yield of other catchments, although the magnitude and sign of the sensitivities may vary under different prevailing climates. We believe that this research

underscores a pressing need for potential impacts of reduced spatial snowpack variability, particularly incorporating climate projection data and remotely sensed snow retrievals.

Data Availability Statement

The data that support the findings of this study are available from the corresponding author upon reasonable request.

References

Barnhart, T. B., Molotch, N. P., Livneh, B., Harpold, A. A., Knowles, J. F., & Schneider, D. (2016). Snowmelt rate dictates streamflow. *Geophysical Research Letters*, *43*(15), 8006-8016.

Barros, A. P., & Lettenmaier, D. P. (1994). Dynamic modeling of orographically induced precipitation. Reviews of Geophysics, 32(3), 265–284. **https://doi.org/10.1029/94RG00625**

Berghuijs, W. R., Woods, R. A., & Hrachowitz, M. (2014). A precipitation shift from snow towards rain leads to a decrease in streamflow. *Nature Climate Change*, *4*(7), 583-586.

Berghuijs, W. R., Woods, R. A., Hutton, C. J., & Sivapalan, M. (2016). Dominant flood generating mechanisms across the United States. *Geophysical Research Letters*, *43*(9), 4382-4390.

Brooks, E. S., Boll, J., & McDaniel, P. A. (2004). A hillslope-scale experiment to measure lateral saturated hydraulic conductivity. *Water Resources Research*, *40*(4).

Caine, N. (1996). Streamflow patterns in the alpine environment of North Boulder Creek, Colorado Front Range. *Zeitschrift für Geomorphologie. Supplementband*, (104), 27-42.

Cayan, D. R. (1996). Interannual climate variability and snowpack in the western United States. *Journal of Climate*, *9*(5), 928-948.

Clifton, A., Rüedi, J. D., & Lehning, M. (2006). Snow saltation threshold measurements in a drifting-snow wind tunnel. *Journal of Glaciology*, *52*(179), 585-596.

Clow, D. W. (2010). Changes in the Timing of Snowmelt and Streamflow in Colorado: A Response to Recent Warming. Journal of Climate, 23(9), 2293–2306. **https://doi.org/10.1175/2009JCLI2951.1**

Deems, J. S., Painter, T. H., Barsugli, J. J., Belnap, J., & Udall, B. (2013). Combined impacts of current and future dust deposition and regional warming on Colorado River Basin snow dynamics and hydrology. In Hydrology and Earth System Sciences (Vol. 17, p. 13). **https://doi.org/10.5194/hess-17-4401-2013**

Doorschot, J. J., Lehning, M., & Vrouwe, A. (2004). Field measurements of snow-drift threshold and mass fluxes, and related model simulations. *Boundary-Layer Meteorology*, *113*(3), 347-368.

Elder, K., Dozier, J., & Michaelsen, J. (1991). Snow accumulation and distribution in an Alpine Watershed. Water Resources Research, 27(7), 1541–1552. **https://doi.org/10.1029/91WR00506**

Erickson, T. A., Williams, M. W., & Winstral, A. (2005). Persistence of topographic controls on the spatial distribution of snow in rugged mountain terrain, Colorado, United States. *Water Resources Research*, *41*(4).

Essery, R., & Etchevers, P. (2004). Parameter sensitivity in simulations of snowmelt. Journal of Geophysical Research: Atmospheres, 109(D20). **https://doi.org/10.1029/2004JD005036**

Essery, R., Li, L., & Pomeroy, J. (1999). A distributed model of blowing snow over complex terrain. HYDROLOGICAL PROCESSES, 13, 16.

Field, C. B., Barros, V. R., Mach, K. J., Mastrandrea, M. D., van Aalst, M., Adger, W. N., ... & Birkmann, J. (2014). *Climate change 2014–Impacts, adaptation and vulnerability: Regional aspects*. Cambridge University Press.

Fontaine, T. A., Cruickshank, T. S., Arnold, J. G., & Hotchkiss, R. H. (2002). Development of a snowfall–snowmelt routine for mountainous terrain for the soil water assessment tool (SWAT). Journal of Hydrology, 262(1), 209–223. **https://doi.org/10.1016/S0022-1694(02)00029-X**

Freudiger, D., Kohn, I., Seibert, J., Stahl, K., & Weiler, M. (2017). Snow redistribution for the hydrological modeling of alpine catchments. *Wiley Interdisciplinary Reviews: Water*, *4*(5), e1232.

Greenland, D. (1989). The Climate of Niwot Ridge, Front Range, Colorado, U.S.A. Arctic and Alpine Research, 21(4), 380. **https://doi.org/10.2307/1551647**

Guyomarc'h, G., & Mérindol, L. (1998). Validation of an application for forecasting blowing snow. Annals of Glaciology, 26, 138–143. **https://doi.org/10.3189/1998AoG26-1-138-143**

Hamlet, A. F., Mote, P. W., Clark, M. P., & Lettenmaier, D. P. (2005). Effects of temperature and precipitation variability on snowpack trends in the western United States. *Journal of Climate*, *18*(21), 4545-4561.

Hartman, M. D., Baron, J. S., Lammers, R. B., Cline, D. W., Band, L. E., Liston, G. E., & Tague, C. (1999). Simulations of snow distribution and hydrology in a mountain basin. Water Resources Research, 35(5), 1587–1603. **https://doi.org/10.1029/1998WR900096**

Hayhoe, K., Wuebbles, D. J., Easterling, D. R., Fahey, D. W., Doherty, S., Kossin, J. P., ... & Wehner, M. F. (2018). Our Changing Climate. Impacts, Risks, and Adaptation in the United States: The Fourth National Climate Assessment, Volume II.

Immerzeel, W. W., Van Beek, L. P., & Bierkens, M. F. (2010). Climate change will affect the Asian water towers. *Science*, *328*(5984), 1382-1385.

Jepsen, S. M., Molotch, N. P., Williams, M. W., Rittger, K. E., & Sickman, J. O. (2012). Interannual variability of snowmelt in the Sierra Nevada and Rocky Mountains, United States: Examples from two alpine watersheds. *Water Resources Research*, *48*(2).

Jones, J. A., Creed, I. F., Hatcher, K. L., Warren, R. J., Adams, M. B., Benson, M. H., ... & Clow, D. W. (2012). Ecosystem processes and human influences regulate streamflow response to climate change at long-term ecological research sites. *BioScience*, *62*(4), 390-404.

Judson, A., & Doesken, N. (2000). Density of Freshly Fallen Snow in the Central Rocky Mountains. Bulletin of the American Meteorological Society, 8(7), 12. **https://doi.org/10.1175/1520-0477(2000)081<1577:DOFFSI>2.3.CO;2**

Kane, D. L., Hinzman, L. D., Benson, C. S., & Liston, G. E. (1991a). Snow hydrology of a headwater Arctic basin: 1. Physical measurements and process studies. Water Resources Research, 27(6), 1099–1109. **https://doi.org/10.1029/91WR00262**

Kane, D. L., Hinzman, L. D., Benson, C. S., & Liston, G. E. (1991b). Snow hydrology of a headwater Arctic basin: 1. Physical measurements and process studies. Water Resources Research, 27(6), 1099–1109. **https://doi.org/10.1029/91WR00262**

Kittel, T. G. F., Williams, M. W., Chowanski, K., Hartman, M., Ackerman, T., Losleben, M., & Blanken, P. D. (2015). Contrasting long-term alpine and subalpine precipitation trends in

a mid-latitude North American mountain system, Colorado Front Range, USA. Plant Ecology & Diversity, 8(5–6), 607–624. **https://doi.org/10.1080/17550874.2016.1143536**

Knowles, J. F., Burns, S. P., Blanken, P. D., & Monson, R. K. (2015). Fluxes of energy, water, and carbon dioxide from mountain ecosystems at Niwot Ridge, Colorado. Plant Ecology & Diversity, 8(5–6), 663–676. **https://doi.org/10.1080/17550874.2014.904950**

Li, L., & Pomeroy, J. W. (1997). Probability of occurrence of blowing snow. Journal of Geophysical Research: Atmospheres, 102(D18), 21955–21964. **https://doi.org/10.1029/97JD01522**

Liston, G. E. (1999). Interrelationships among Snow Distribution, Snowmelt, and Snow Cover Depletion: Implications for Atmospheric, Hydrologic, and Ecologic Modeling. Journal of Applied Meteorology, 38(10), 1474–1487. **https://doi.org/10.1175/1520-0450(1999)038<1474:IASDSA>2.0.CO;2**

Livneh, B., & Badger, A. M. (2020). Drought less predictable under declining future snowpack. *Nature Climate Change*, *10*(5), 452-458.

Livneh, B., Deems, J. S., Schneider, D., Barsugli, J. J., & Molotch, N. P. (2014). Filling in the gaps: Inferring spatially distributed precipitation from gauge observations over complex terrain. *Water Resources Research*, *50*(11), 8589-8610.

Livneh, B., Deems, J., Buma, B., Barsugli, J., Schneider, D., Molotch, N., Wolter, K., & Wessman, C. A. (2015). Catchment Response to Bark Beetle Outbreak and Dust-on-Snow in the Colorado Rocky Mountains. Journal of Hydrology, 523. **https://doi.org/10.1016/j.jhydrol.2015.01.039**

Luce, C. H., Tarboton, D. G., & Cooley, K. R. (1998). The influence of the spatial distribution of snow on basin-averaged snowmelt. Hydrological Processes, 12(10–11), 1671–1683. **https://doi.org/10.1002/(SICI)1099-1085(199808/09)12:10/11<1671::AID-HYP688>3.0.CO;2-N**

Luce, C. H., Tarboton, D. G., & Cooley, K. R. (1999). Sub-grid parameterization of snow distribution for an energy and mass balance snow cover model. Hydrological Processes, 13(12–13), 1921–1933. **https://doi.org/10.1002/(SICI)1099-1085(199909)13:12/13<1921::AID-HYP867>3.0.CO;2-S**

Marks, D., Link, T., Winstral, A., & Garen, D. (2001). Simulating snowmelt processes during rain-on-snow over a semi-arid mountain basin. Annals of Glaciology, 32, 195–202. **https://doi.org/10.3189/172756401781819751**

McCabe, G. J., Clark, M. P., & Hay, L. E. (2007). Rain-on-Snow Events in the Western United States. Bulletin of the American Meteorological Society, 88(3), 319–328. **https://doi.org/10.1175/BAMS-88-3-319**

McKay, M. D., Beckman, R. J., & Conover, W. J. (1979). Comparison of three methods for selecting values of input variables in the analysis of output from a computer code. Technometrics, 21(2), 239-245.

McGuire, C. R., Nufio, C. R., Bowers, M. D., & Guralnick, R. P. (2012). Elevation-Dependent Temperature Trends in the Rocky Mountain Front Range: Changes over a 56- and 20-Year Record. PLOS ONE, 7(9), e44370. **https://doi.org/10.1371/journal.pone.0044370**

Moriasi, D. N., Arnold, J. G., Van Liew, M. W., Bingner, R. L., Harmel, R. D., & Veith, T. L. (2007). Model evaluation guidelines for systematic quantification of accuracy in watershed simulations. *Transactions of the ASABE*, *50*(3), 885-900.

Mote, P. W., Hamlet, A. F., Clark, M. P., & Lettenmaier, D. P. (2005). Declining mountain snowpack in western North America. *Bulletin of the American meteorological Society*, *86*(1), 39-50.

Musselman, K. N., Clark, M. P., Liu, C., Ikeda, K., & Rasmussen, R. (2017). Slower snowmelt in a warmer world. *Nature Climate Change*, *7*(3), 214-219.

Pomeroy, J. W. (1991). Transport and sublimation of snow in wind-scoured alpine terrain. *Snow, Hydrology and Forests in Alpine Areas, edited by: Bergman, H., Lang, H., Frey, W., Issler, D., and Salm, B., IAHS Press*, *205*, 131-140.

Pomeroy, J. W., Toth, B., Granger, R. J., Hedstrom, N. R., & Essery, R. L. H. (2003). Variation in surface energetics during snowmelt in a subarctic mountain catchment. Journal of Hydrometeorology, 4(4), 702–719. **https://doi.org/10.1175/1525-7541(2003)004<0702:VISEDS>2.0.CO;2**

Raleigh, M. S., Livneh, B., Lapo, K., & Lundquist, J. D. (2016). How does availability of meteorological forcing data impact physically based snowpack simulations?. *Journal of hydrometeorology*, *17*(1), 99-120.

Rajagopalan, B., Nowak, K., Prairie, J., Hoerling, M., Harding, B., Barsugli, J., ... & Udall, B. (2009). Water supply risk on the Colorado River: Can management mitigate?. *Water Resources Research*, *45*(8).

Stewart, I. T. (2009). Changes in snowpack and snowmelt runoff for key mountain regions. Hydrological Processes, 23(1), 78–94. **https://doi.org/10.1002/hyp.7128**

Teufel, B., Diro, G. T., Whan, K., Milrad, S. M., Jeong, D. I., Ganji, A., ... & Sushama, L. (2017). Investigation of the 2013 Alberta flood from weather and climate perspectives. *Climate Dynamics*, *48*(9), 2881-2899.

Vano, J. A. (2020). Implications of losing snowpack. *Nature Climate Change*, *10*(5), 388-390.

Viviroli, D., Dürr, H. H., Messerli, B., Meybeck, M., & Weingartner, R. (2007). Mountains of the world, water towers for humanity: Typology, mapping, and global significance. *Water resources research*, *43*(7).

Westrick, K. J., & Mass, C. F. (2001). An evaluation of a high-resolution hydrometeorological modeling system for prediction of a cool-season flood event in a coastal mountainous watershed. *Journal of Hydrometeorology*, *2*(2), 161-180.

Whitaker, A., Alila, Y., Beckers, J., & Toews, D. (2003). Application of the distributed hydrology soil vegetation model to Redfish Creek, British Columbia: model evaluation using internal catchment data. *Hydrological processes*, *17*(2), 199-224.

Wigmosta, M. S., Vail, L. W., & Lettenmaier, D. P. (1994). A distributed hydrology-vegetation model for complex terrain. *Water resources research*, *30*(6), 1665-1679.

Williams, M. W., Losleben, M., Caine, N., & Greenland, D. (1996). Changes in climate and hydrochemical responses in a high-elevation catchment in the Rocky Mountains, USA. *Limnology and Oceanography*, *41*(5), 939-946.

Winstral, A., Elder, K., & Davis, R. E. (2002). Spatial Snow Modeling of Wind-Redistributed Snow Using Terrain-Based Parameters. Journal of Hydrometeorology, 3(5), 524–538. **https://doi.org/10.1175/1525-7541(2002)003<0524:SSMOWR>2.0.CO;2**

Xia, Y., Fabian, P., Stohl, A., & Winterhalter, M. (1999). Forest climatology: estimation of missing values for Bavaria, Germany. *Agricultural and Forest Meteorology*, *96*(1-3), 131-144.

Tables

Table 1. Description and sources of static model inputs.

Data	***Notes***	***Source***
DEM	Sampled 10-m resolution domain to produce 20-m DEM for DHSVM	U.S. Geological Survey, 2017, 1/3rd arc-second Digital Elevation Models (DEMs) - USGS National Map 3DEP Downloadable Data Collection: U.S. Geological Survey.
Soil Types	Nearest neighbor interpolation from native 20-m SSURSGO data	Soil Survey Staff, Natural Resources Conservation Service, United States Department of Agriculture. Web Soil Survey. Available online at https://websoilsurvey.nrcs.usda.gov/.
Vegetation	Nearest neighbor interpolation from native 10-m grid	Cline, D. 2019. Green Lakes Valley land cover classification, Niwot Ridge LTER, Colorado ver 2. Environmental Data Initiative. https://doi.org/10.6073/pasta/a585afc617269ce06652c559ffde2688
Geology	Resampled to match 20-m DHSVM grid	Cole, J.C., and Braddock, W.A., 2009, Geologic map of the Estes Park 30’ x 60’ quadrangle, north-central Colorado: U.S. Geological Survey Scientific Investigations Map 3039

Table 2. The five Niwot Ridge LTER observation stations and streamflow gage used in this study with their respective latitude, longitude and elevation.

Name	***Latitude (°)***	***Longitude (°)***	***Elevation (m)***
Arikaree	40.049	-105.640	3798
D1	40.059	-105.616	3743
GL4	40.056	-105.617	3560
Saddle	40.049	-105.592	3525
TVan	40.053	-105.586	3480
Streamflow Gage	40.049	-105.617	3560

Table 3: characteristics of each level of uniformity analyzed in this study, including the uniformity, U, the spatial standard deviation and spatial mean SWE for each case. We note that smaller values of U correspond with greater snowpack spatial uniformity.

Scenario	U (unitless)	Standard deviation of SWE (m)	Mean SWE (m)
Control	1.137	0.651	0.573
1/6	0.947	0.543	0.573
2/6	0.758	0.434	0.573
3/6	0.568	0.326	0.573
4/6	0.379	0.217	0.573
5/6	0.189	0.109	0.573
Uniform	0.000	0.000	0.573

Figure Legends

Figure 1. Map of the Green Lakes Valley catchment (outlined in black) within the Niwot Ridge LTER, shaded by elevation. Regional location of the Green Lakes Valley within the Western United States is shown in the inset. Locations of meteorological stations used to provide the DHSVM forcing data are shown (colored dots).

Figure 2. Maps of (a) the mean SWE reconstruction product for the Green Lakes Valley catchment (Jepsen et al., 2012), (b-f) increasing iterations of redistributed mean SWE, and (g) mean SWE distributed uniformly over the catchment.

Figure 3. Basin averaged May 1st SWE (blue) and total precipitation accumulated from May to September (gray) for each water year of the period of analysis (2001-2014). Dashed lines of the coinciding colors represent the median value for all of the years of record for both SWE and precipitation.

Figure 4. Results from the control and snow-redistribution simulations with May through September precipitation forcing included. (A) Multi-annual mean of DHSVM simulated cumulative runoff (red) and basin averaged SWE (blue) from the control simulation are shown with solid lines. Uncertainty bands show the 95% confidence interval for daily mean runoff and SWE for all years in the period of analysis (2001-2014). For each time step, confidence intervals were calculated from an empirically bootstrapped, 1000-member ensemble of daily SWE and runoff resampled from the simulations. Day-of-year mean SWE/runoff were calculated for each of the 1000 ensemble members, and, for each day of the year, the 2.5^{th} and 97.5^{th} percentiles of the distribution of daily, bootstrapped means are shown as the bounding lines of the uncertainty bands. (B) Multi-annual mean SWE anomalies compared to the control simulations for each of the redistributed SWE simulations (colored lines) with uncertainty bands derived using the method described above. Vertical dashed lines, consistently colored by simulation, indicate the mean date of snowpack melt out for all years. (C) Multi-annual mean cumulative runoff anomalies compared to the control simulations for each of the redistributed simulations (colored lines) with uncertainty bands derived using the method described above. Horizontal lines along the right-hand vertical axis, consistently colored by simulation, indicate mean cumulative runoff for all years of analysis.

Figure 5. Results from the control and snow-redistribution simulations with May through September precipitation forcing excluded. (A) Multi-annual mean of DHSVM simulated cumulative runoff (red) and basin averaged SWE (blue) from the control simulation are shown with solid lines. Uncertainty bands show the 95% confidence interval for daily mean runoff and SWE for all years in the period of analysis (2001-2014). Confidence intervals are calculated using the same method as described in the caption of Figure 4. (B) Multi-annual mean SWE anomalies compared to the control simulations for each of the redistributed SWE simulations (colored lines) with uncertainty bands derived using the method described above. Vertical dashed lines, consistently colored by simulation, indicate the mean date of snowpack melt out for all years. (C) Multi-annual mean cumulative runoff anomalies compared to the control simulations for each of the redistributed SWE simulations (colored lines) with uncertainty bands

derived using the method described above. Horizontal lines along the right-hand vertical axis, consistently colored by simulation, indicate mean cumulative runoff for all years of analysis.

Figure 6. Annual May 1st SWE (horizontal axis) compared to the simulated annual cumulative runoff normalized by the control experiment for the year of the simulation (vertical axis) for all years within the period of analysis (2001-2014). Each vertical line of dots represents the control and SWE redistributed simulations for a single year with May through September precipitation excluded. Values of normalized cumulative runoff less than 1 indicate a decrease in the total simulated streamflow compared to the control simulation.

Figure 7. (A) DHSVM simulated cumulative runoff (red) and basin averaged SWE (blue) from simulations with the randomized variations of the control initial condition. (B) SWE anomalies compared to the control simulations for each of the randomized SWE simulations at different levels of spatial uniformity (colored lines). Vertical dashed lines (colored by simulation) denote the date of snowpack melt out for each simulation. (C) Cumulative runoff anomalies compared to the control simulations for each of the randomized and redistributed SWE simulations (colored lines). Horizontal lines along the right-hand vertical axis indicate the total cumulative runoff rather than the anomaly.

Figure 8. (Upper panel) Difference in the multi-annual mean of snowmelt (depth) from the uniformly distributed SWE simulation compared to the control simulation. The red dashed line shows the inflection point where the difference between the two simulations changes signs. (Lower panel) Mean differences in the snowmelt (rate), runoff (rate), soil moisture (depth) and the water table depth from the uniformly distributed SWE simulation compared to the control simulation. Periods for which the means (and subsequent differences) are derived are divided by the location of the red dashed line.

Appendix Figures

Figure A1. Observed (black) streamflow for the daily cycle from 2001 to 2014. The selected parameter set is highlighted in red, while the grey shaded area depicts the range of streamflow simulated from the Monte Carlo parameter selection. The top panel shows the daily average streamflow, whereas the bottom panel shows all days during the study period where missing data for the observations, denoted by gaps in the black line.

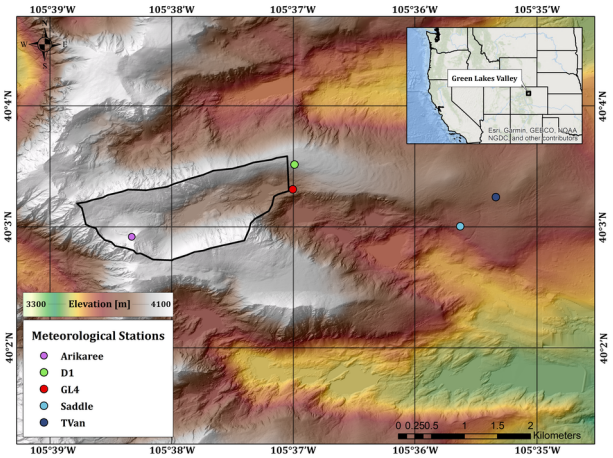

HYP_14331_Figure1_new.tif

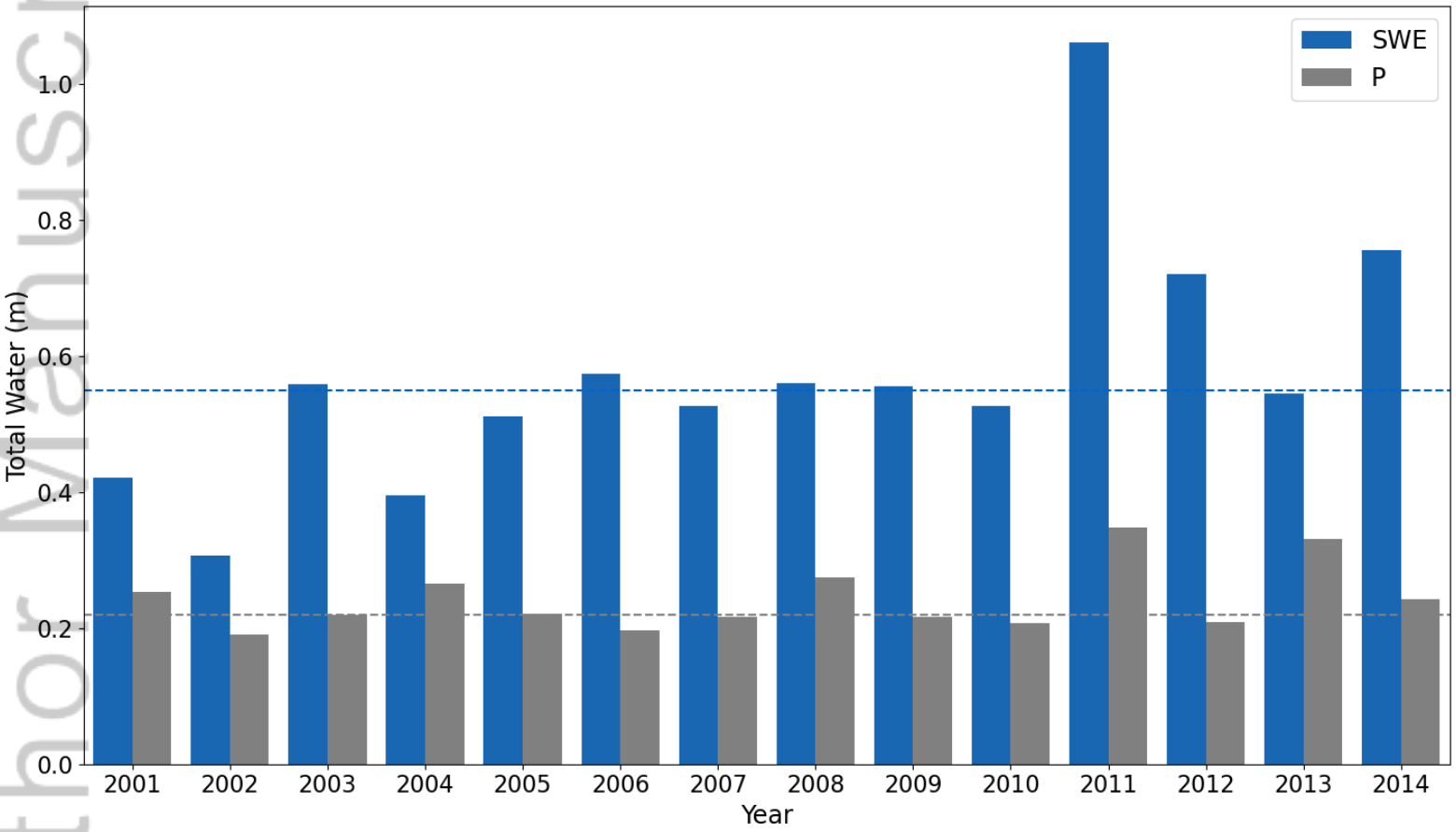

HYP_14331_Figure3_new.tif

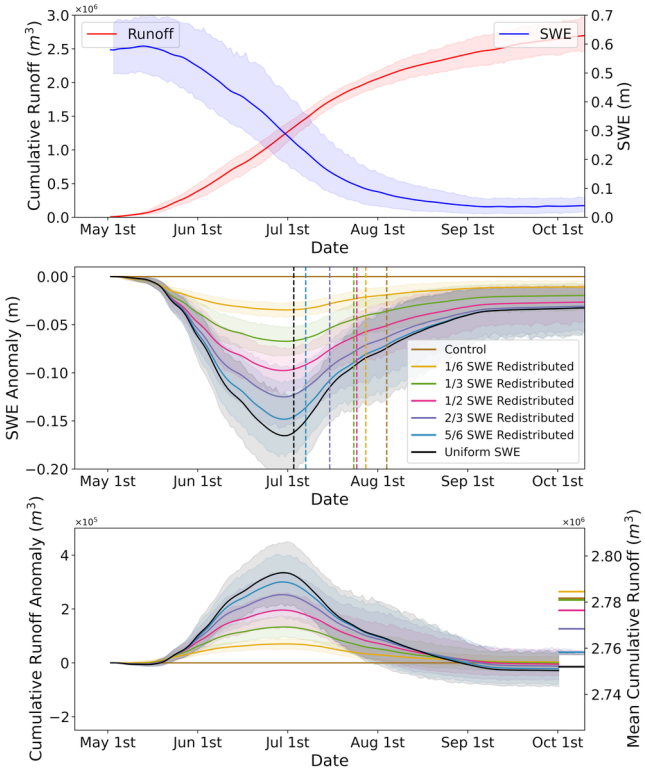

HYP_14331_Figure4_new.tif

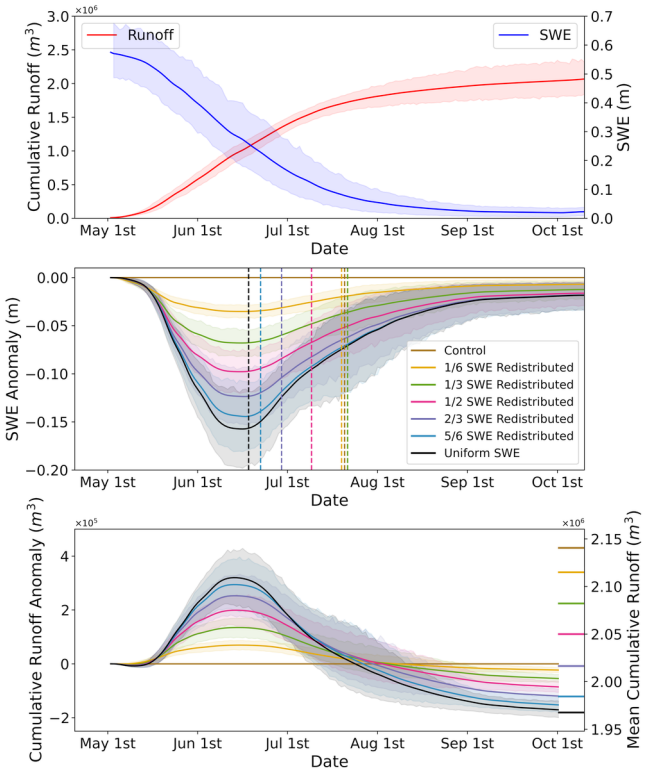

HYP_14331_Figure5_new.tif

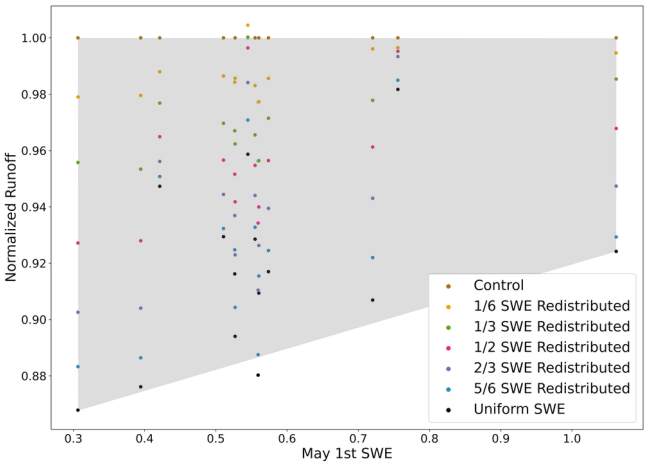

HYP_14331_Figure6_new.tif

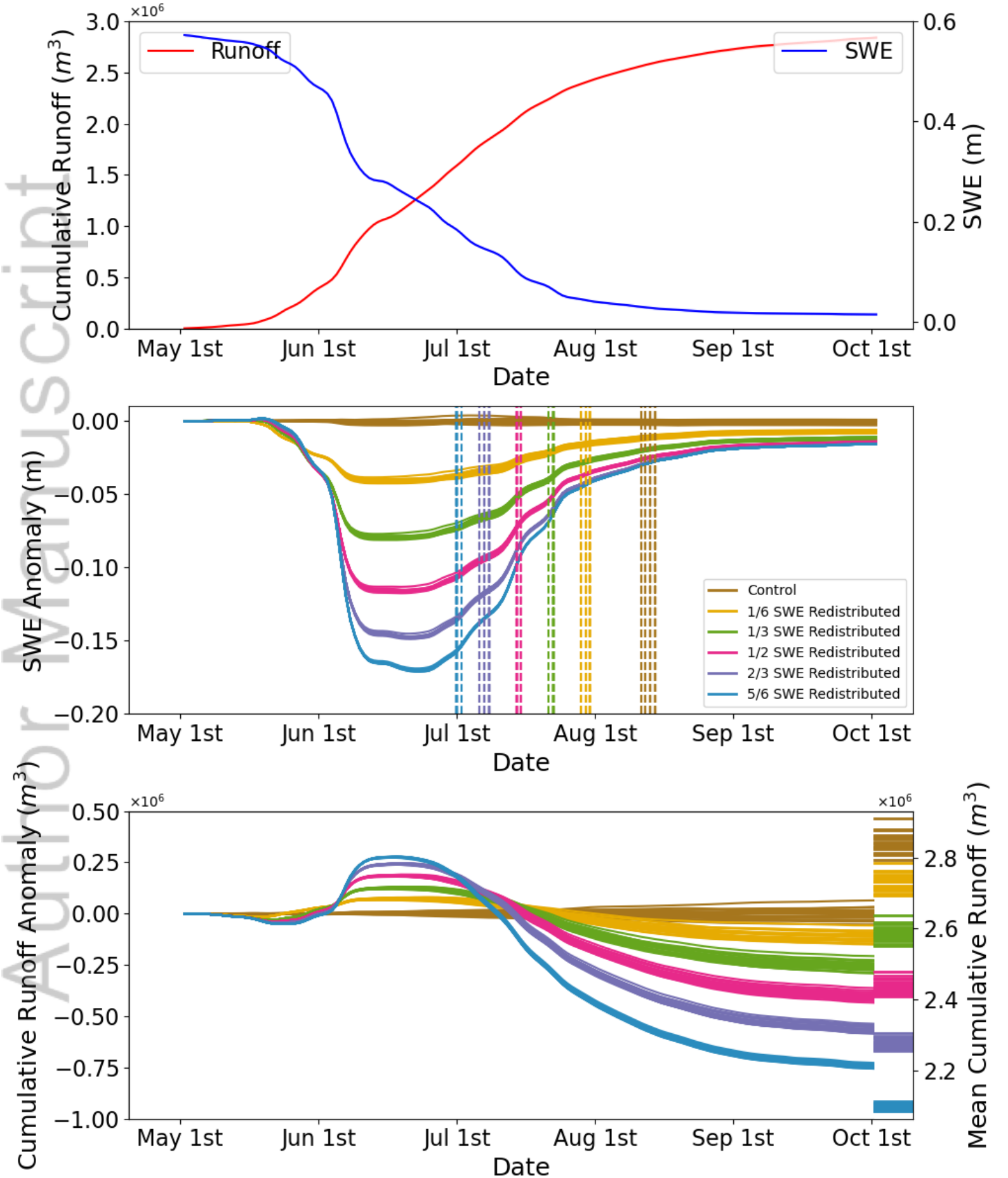

HYP_14331_Figure7_new.tif

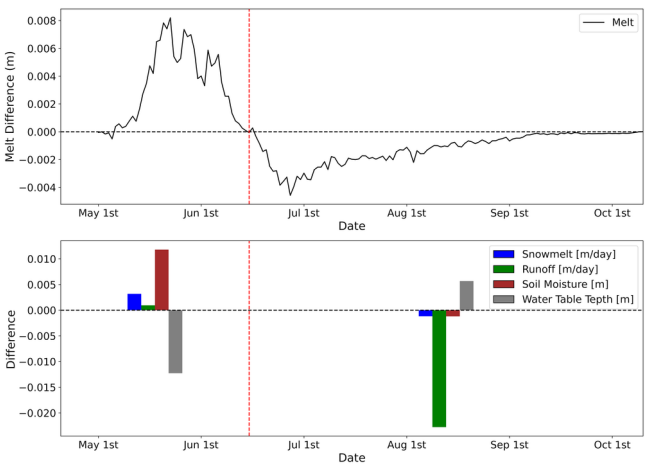

HYP_14331_Figure8_new.tif

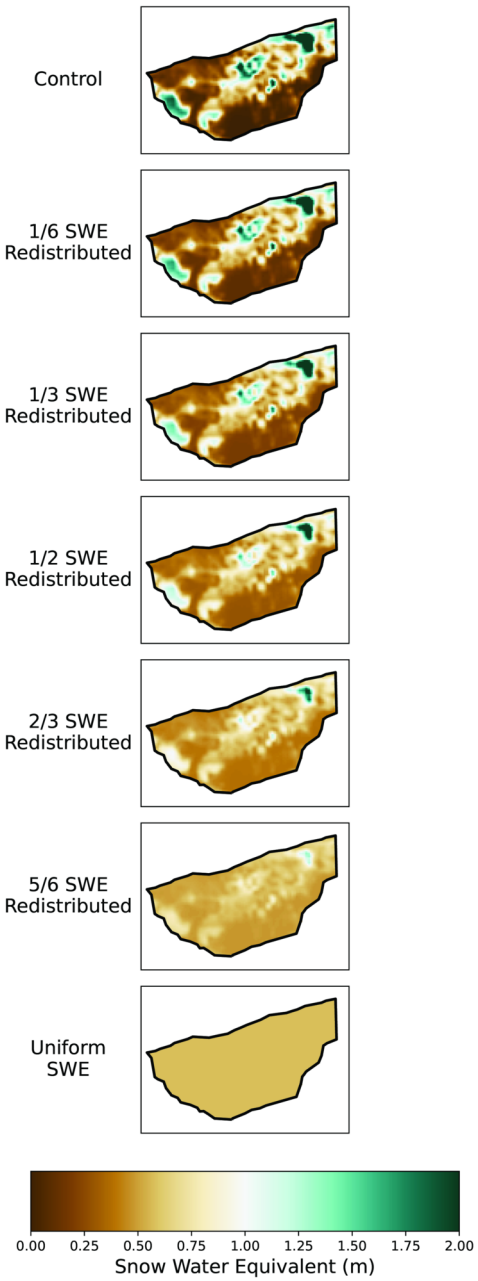

HYP_14331_Figure_2.tif

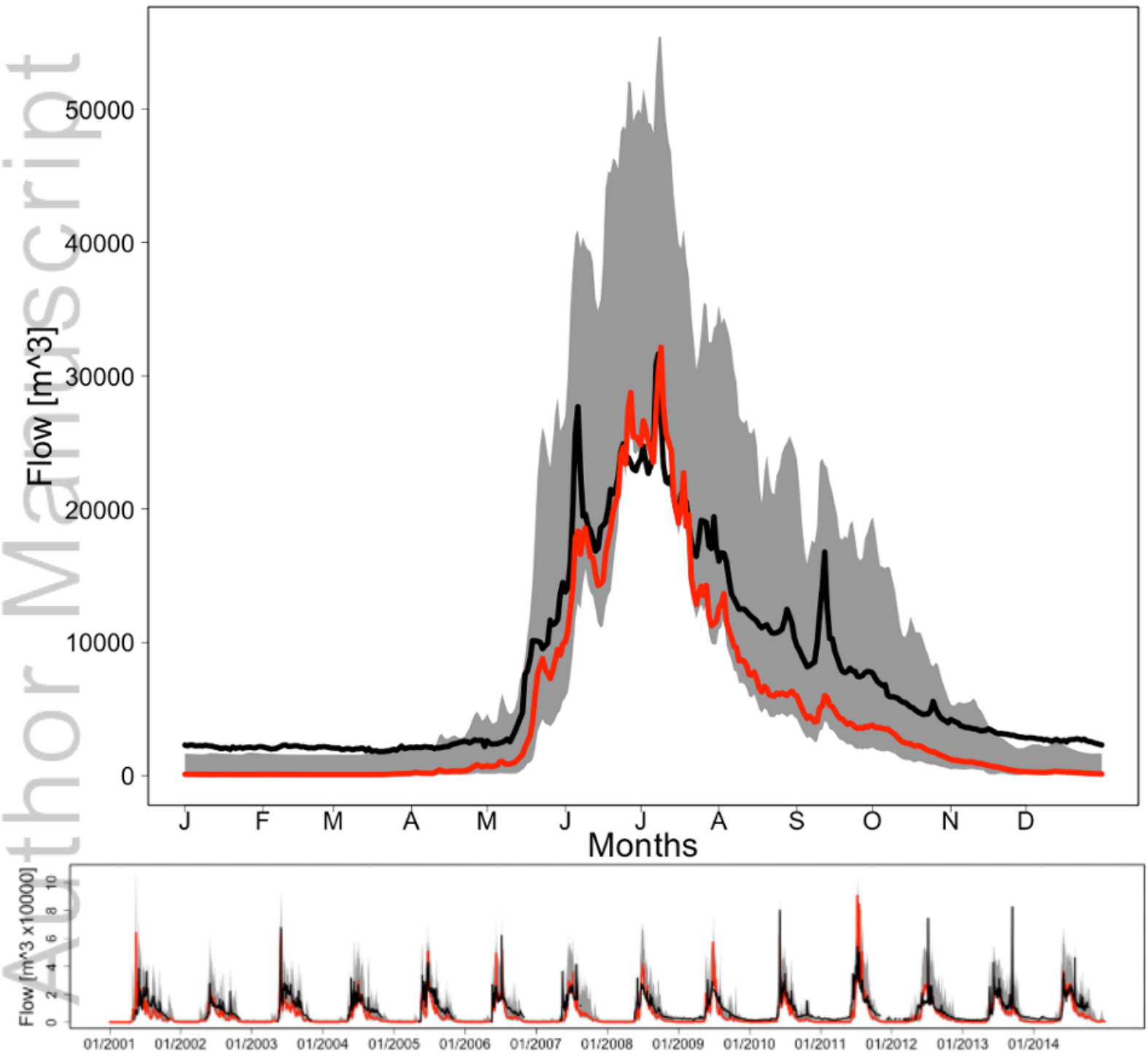

HYP_14331_Figure_A1.tif

We evaluate the implications of scenarios where snow becomes more uniformly distributed due to increases in density and reduced wind redistribution as hypothesized under future warming. Hydrologic model results indicate decreases in streamflow resulting from greater exposure of more uniform snowpack to the atmosphere and solar inputs. The sensitivity of uniform snowpacks are greater for shallow snow cover, with implications for climate change.

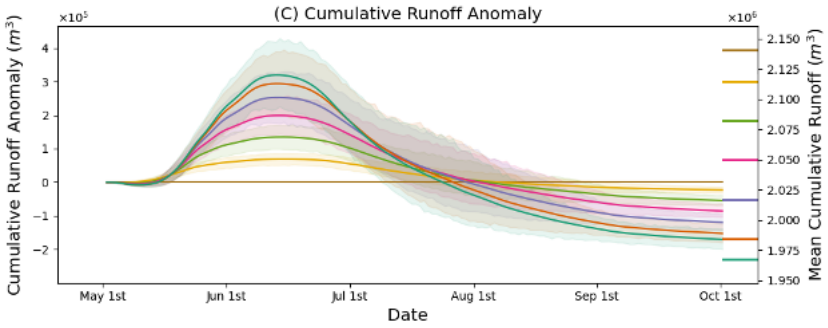

The sensitivity of runoff generation to snowpack uniformity in an alpine watershed: Green Lakes Valley, Niwot Ridge Long Term Ecological Research Station

Andrew M. Badger, Nels Bjarke, Noah P. Molotch, and Ben Livneh